AD_____

Award Number: W81XWH-08-1-0367

TITLE: Regulatory role of the NF-kB pathway in lymphangiogenesis and breast cancer mestatasis

PRINCIPAL INVESTIGATOR: Michael Flister

CONTRACTING ORGANIZATION: Southern Illinois University
Springfield, IL, 62702

REPORT DATE: July 2009

TYPE OF REPORT: Annual Summary

PREPARED FOR: U.S. Army Medical Research and Materiel Command
Fort Detrick, Maryland 21702-5012

DISTRIBUTION STATEMENT: Approved for Public Release;
Distribution Unlimited

REPORT DOCUMENTATION PAGE

Form Approved
OMB No. 0704-0188

1. REPORT DATE	2. REPORT TYPE	3. DATES COVERED
07/31/2009	Annual Summary	1 Jul 2008 – 30 Jun 2009

4. TITLE AND SUBTITLE
Regulatory role of the NF-kB pathway in lymphangiogenesis and breast cancer metastasis

5a. CONTRACT NUMBER
W81XWH-08-1-0367

5b. GRANT NUMBER

5c. PROGRAM ELEMENT NUMBER

6. AUTHOR(S)

Mike Flister

Email: mflister@siumed.edu

5d. PROJECT NUMBER

5e. TASK NUMBER

5f. WORK UNIT NUMBER

7. PERFORMING ORGANIZATION NAME(S) AND ADDRESS(ES)
Southern Illinois University
Springfield, IL, 62702

8. PERFORMING ORGANIZATION REPORT NUMBER

9. SPONSORING / MONITORING AGENCY NAME(S) AND ADDRESS(ES)
U.S. Army Medical Research and Materiel Command
Fort Detrick, Maryland 21702-5012

10. SPONSOR/MONITOR'S ACRONYM(S)

11. SPONSOR/MONITOR'S REPORT NUMBER(S)

12. DISTRIBUTION / AVAILABILITY STATEMENT
Approved for Public Release; Distribution Unlimited

13. SUPPLEMENTARY NOTES

14. ABSTRACT

The concept of inflammation-induced lymphangiogenesis (i.e., formation of new lymphatic vessels) has long been recognized, but the molecular mechanisms remained largely unknown. The two primary mediators of lymphangiogenesis are vascular endothelial growth factor receptor-3 (VEGFR-3) and Prox1. The key factors that regulate inflammation-induced transcription are members of the NF-κB family; however, the role of NF-κB in regulation of lymphatic-specific genes has not been defined. Here, we identified VEGFR-3 and Prox1 as downstream targets of the NF-κB pathway. In vivo time-course analysis of inflammation-induced lymphangiogenesis showed activation of NF-κB followed by sequential upregulation of Prox1 and VEGFR-3 that preceded lymphangiogenesis by 4 and 2 days, respectively. Activation of NF-κB by inflammatory stimuli also elevated Prox1 and VEGFR-3 expression in cultured lymphatic endothelial cells resulting in increased proliferation and migration. We also show that Prox1 synergizes with the p50 of NF-κB to control VEGFR-3 expression. Collectively, our findings suggest that induction of the NF-κB pathway by inflammatory stimuli activates Prox1, and both NF-κB and Prox1 activate the VEGFR-3 promoter leading to increased receptor expression in lymphatic endothelial cells. This, in turn, enhances the responsiveness of pre-existing lymphatic endothelium to VEGFR-3 binding factors, VEGF-C and VEGF-D, ultimately resulting in robust lymphangiogenesis.

15. SUBJECT TERMS
Breast cancer metastasis; Lymphatic; Lymphangiogenesis; Vascular endothelial growth factor receptor-3 (VEGFR-3); Prospero-related homeobox-1 (Prox1); Inflammation; Nuclear factor-kappa B (NF-κB)

16. SECURITY CLASSIFICATION OF:			17. LIMITATION OF ABSTRACT	18. NUMBER OF PAGES	19a. NAME OF RESPONSIBLE PERSON
					USAMRMC
a. REPORT	b. ABSTRACT	c. THIS PAGE			19b. TELEPHONE NUMBER *(include area code)*
U	U	U	UU	33	

Standard Form 298 (Rev. 8-98)
Prescribed by ANSI Std. Z39.18

Table of Contents

Page

Introduction……..……..5

Body……..7

Key Research Accomplishments……..22

Reportable Outcomes……23

Conclusion……24

References……25

Appendices……30

Introduction:

Chronic inflammation is frequently associated with breast cancer development[1;2], progression, and metastasis, which is the leading cause of mortality in these patients[3]. Frequently, the formation of new lymphatic vessels, i.e., lymphangiogenesis, facilitates initial metastasis to regional lymph nodes. Strong correlative evidence links chronic inflammation to both increased lymphangiogenesis[4] and breast cancer metastasis[5], but the direct mechanism(s) are largely unknown. The key protein that regulates lymphangiogenesis is vascular endothelial growth factor receptor-3 (VEGFR-3)[6], a tyrosine kinase receptor expressed primarily in lymphatic endothelial cells (LECs)[7]. VEGFR-3 signaling is activated upon binding of vascular endothelial growth factor (VEGF)-C or the related factor, VEGF-D[6]. In adulthood, lymphangiogenesis and elevated VEGFR-3 expression coincide with pro-inflammatory conditions including cancer[8], wound healing[9], and chronic inflammatory diseases. Increased lymphatic vessel density has been documented in chronic airway infection[10], psoriasis[11], arthritis[12] and corneal injury[13]. VEGF-C and VEGF-D are elevated during inflammation, being produced by a variety of cells residing at inflamed sites, including macrophages[10;14;15], dendritic cells, neutrophils[10], mast cells, fibroblasts[16] and tumor cells[15]. Inflammation-induced lymphatic hyperplasia and lymphangiogenesis are likely the result of increased VEGFR-3 expression that amplifies response to VEGF-C/-D. This is supported by observations that blocking VEGFR-3 signaling inhibits lymphangiogenesis during chronic inflammation[10], wound healing[17], and malignancy[18]. Lymphangiogenesis is also regulated by the lymphatic-specific transcription factor, Prospero-related homeobox-1 (Prox1)[19;20] that specifies lymphatic endothelial cell-fate by regulating VEGFR-3[20] and other lymphatic-specific proteins during embryogenesis. The central role of Prox1 in developmental lymphangiogenesis suggests a similar role for Prox1 in adulthood. Studies have shown that Prox1 induces VEGFR-3 expression in adult blood vascular endothelial cells (BECs)[19;21], whereas silencing Prox1 in adult LECs downregulates VEGFR-3 expression[21;22]. Prox1 has been shown to be upregulated by inflammatory cytokines[23] and to colocalize with VEGFR-3 in lymphatic vessels. However, the role of Prox1 in regulation of VEGFR-3 expression during inflammation *in vivo* is unknown. The primary mediators of the intracellular response to inflammation are dimeric transcription factors that belong to the nuclear factor-kappaB (NF-κB) family consisting of RelA (p65), NF-κB1 (p50), RelB, c-Rel, and NF-κB2 (p52)[24]. The main NF-κB protein

complexes that regulate the transcription of responsive genes are p50/p65 heterodimers or p50 and p65 homodimers[25]. Over 450 NF-κB inducible genes have been identified, including proteins that mediate inflammation, immunity, tumorigenesis, and angiogenesis[24]. Several NF-κB-regulated genes stimulate lymphangiogenesis either directly (e.g., VEGF-A[26] and VEGF-C[27]) or indirectly, by upregulating VEGF-C and VEGF-D (e.g., IL-1β[16], TNF-α[16]and COX-2[15]). Activated NF-κB signaling coincides with increased VEGFR-3^{+} lymphatics during inflammation[10]suggesting a role for NF-κB in regulation of VEGFR-3 expression. In the work supported by this proposal we have identified one of the central molecular mechanisms underlying inflammation- and tumor-induced lymphangiogenesis. Our current data, based on *in vivo* and *in vitro* models of inflammation, suggest that Prox1 and VEGFR-3 are directly regulated by inflammation through NF-κB signaling. These important and novel findings have set the basis for future studies that will investigate the primary functions of these factors in promoting breast cancer lymphatic metastasis.

Body

Task 1. To determine the synergistic effects of inflammatory mediators (TNF-α, IL-1β, and IL-6) on proliferation, migration and survival of lymphatic endothelial cells (LEC) induced by VEGFR-3 ligands in vitro. To accomplish this task, we will:

A. Measure effect of lymphangiogenic factors VEGF-C (50ng/ml) or VEGF-D (50ng/ml) on induction of LEC proliferation in the presence or absence of TNF-α (10ng/ml), IL-1β (10ng/ml), or IL-6 (10ng/ml).
B. Measure effect of lymphangiogenic factors VEGF-C (50ng/ml) or VEGF-D (50ng/ml) on LEC migration in the presence or absence of TNF-α (10ng/ml), IL-1β (10ng/ml), or IL-6 (10ng/ml).
C. Measure effect of lymphangiogenic factors VEGF-C (50ng/ml) or VEGF-D (50ng/ml) on LEC survival in the presence or absence of TNF-α (10ng/ml), IL-1β (10ng/ml), or IL-6 (10ng/ml).

Data toward accomplishment of Task 1:

In this report we have accomplished the following preliminary studies necessary for completion of the goals outlined in Task 1:

- cloned and characterized the human VEGFR-3 promoter
- demonstrated that NF-κB subunits p50 and p65 directly activate the VEGFR-3 promoter
- showed that NF-κB dependent inflammatory stimuli, IL-3 and LPS, upregulate endogenous VEGFR-3 expression in cultured LECs
- demonstrated that IL-3 and LPS induce LEC proliferation and migration
- showed that pretreatment with IL-3 and LPS enhances LEC proliferation and migration that is induced by the VEGFR-3 specific ligand, VEGF-C152S
- determined that NF-κB signaling is necessary for endogenous VEGFR-3 gene expression in LECs using sequence-specific and pharmacological NF-κB inhibitors

Collectively, we have found that inflammation-induced NF-κB signaling directly activates the VEGFR-3 promoter. We hypothesize that this, in turn, increases VEGFR-3 receptor density that leads to greater activation by VEGFR-3 ligands, VEGF-C and VEGF-D, resulting in a more robust lymphangiogenic response. Detailed methods for the following section of this report are found in Appendix 1.

Characterization of the human VEGFR-3 regulatory elements

As previously described in the traineeship proposal (BC073318), we have cloned and characterized the human VEGFR-3 promoter. Previous testing of the mouse VEGFR-3 promoter[28]demonstrated that the proximal 0.8kb is sufficient to mediate cell-type-specific transcriptional activity. Within this promoter region sequence analysis software predicted numerous consensus NF-κB binding sites that were conserved in mouse, rat, and human VEGFR-3 promoters. This suggested that VEGFR-3 expression may be regulated by these factors; however, NF-κB and Prox1 dependent regulation of the human, rat, or mouse promoter has not been previously examined.

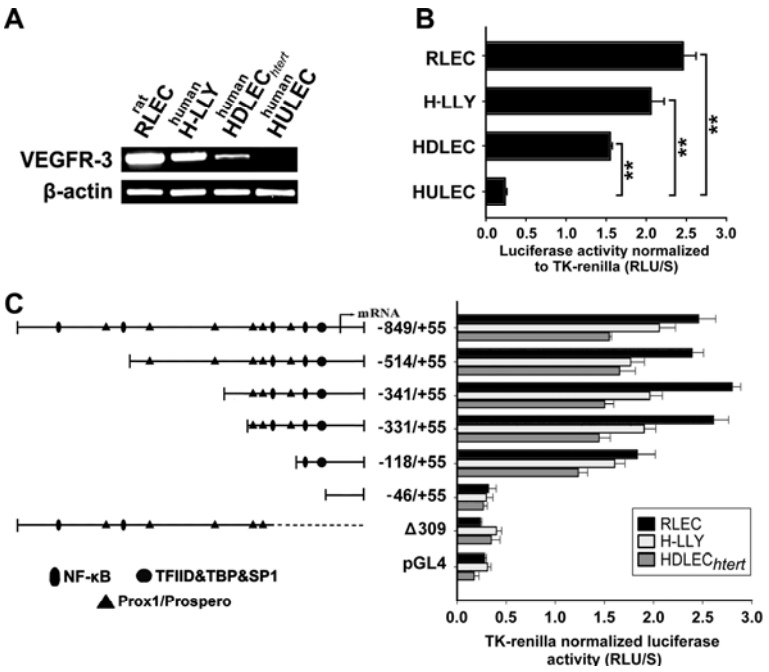

Figure 1. VEGFR-3 promoter characterization and gene expression in lymphatic endothelial cells. (A) VEGFR-3 mRNA expression and (B) full-length VEGFR-3$^{-849/+55}$ promoter activity were measured in the lymphatic endothelial cell lines RLEC, H-LLY and HDLEC$_{htert}$. Human lung blood microvascular endothelial cell line, HULEC, was used as a VEGFR-3 negative cell line. Data shown are a representative image of VEGFR-3 transcript expression of three independent experiments (A) and the mean promoter activity of three independent experiments ± SEM (B). ** indicates *P*<.01 vs. VEGFR-3 expression in the negative control cell line HULEC as determined by Student's unpaired t-test. (C) Activities of VEGFR-3 promoter deletion constructs were tested in RLEC, H-LLY and HDLEC$_{htert}$. The left panel shows schematic illustration of deletion constructs with relative locations of predicted transcription factor binding sites. The right panel shows VEGFR-3 promoter activity of deletion constructs presented as relative light units per second (RLU/S) normalized per renilla luciferase activity of co-transfected thymidine kinase (TK)-renilla plasmid. Experiments were performed in duplicate and reproduced at least three times. Data are presented as the mean promoter activity of three independent experiments + SEM

High luciferase activity of the VEGFR-3$^{-849/+55}$ promoter was detected in three LEC lines with endogenous VEGFR-3 expression (Figure 1A). Promoter activity in LECs was significantly higher by 10.25±0.7- (RLEC), 8.6±0.7- (H-LLY), and 6.5±0.2-fold (HDLEC$_{htert}$) as compared with the human blood vascular endothelial line, HULEC (Figure 1B). Promoter-reporter specificity was also confirmed by empty vector and a promoter construct lacking the transcription start site (Δ309), both of which had 10% of the activity mediated by full-length VEGFR-3$^{-849/+55}$ (Figure 1C).

To identify the core elements required for transcriptional activity of the promoter we performed deletion analysis. Truncation from -849bp to -331bp did not significantly affect promoter activity (Figure 3C), suggesting that cis-acting response elements are located within the proximal -331/+55bp region. Similar promoter activity was measured in human and rat LECs suggesting that the regulatory elements are conserved among species. Analysis of the -331/+55bp region identified putative binding sites for several transcription factors including NF-κB and Prox1. Promoter truncation from -331bp to -118bp reduced activity

by 15-30% while reduction to -46bp reduced luciferase activity to the level of control Δ309 construct (Figure 1C). This suggested that NF-κB and Prox1, whose binding sites are located within the proximal -331bp region, are potentially responsible for the regulation of VEGFR-3 expression observed *in vivo*.

NF-κB transcription factors directly activate the VEGFR-3 promoter in LECs

The primary goals of this proposal were two-fold: **1)** to identify factors regulating VEGFR-3 gene expression and **2)** to determine the role of these factors in lymphangiogenesis associated with breast cancer and tumor-derived inflammation. Members or the NF-κB family of transcription factors (e.g. p50 and p65 subunits) are the primary intracellular mediators of inflammation and are frequently constitutively active in the tumor microenvironment. The well documented roles of NF-κB in tumor progression, lymphangiogenesis, and lymphatic metastasis along with the aforementioned VEGFR-3 promoter characterization, strongly suggest that NF-κB may regulate the VEGFR-3 promoter directly. To answer whether NF-κB regulates VEGFR-3 expression, LEC were co-transfected with the VEGFR-3$^{-849/+55}$ promoter and pCMV-Flag-p50, pCMV-Flag-p65, or empty plasmids. Equivalent expression of NF-κB subunits was determined by Western blot using Flag-specific antibody (Figure 2A). NF-κB p65 activated VEGFR-3 promoter by 9±1.0- and 6±0.5-fold in H-LLY and RLEC, respectively, compared with empty-vector. However, NF-κB p50 increased promoter activity by 58±7- and 51±5-fold in H-LLY and RLEC (Figure 3A). The difference in promoter activation was not due to functional deficiency of Flag-p65 construct as demonstrated by co-transfection with a NF-κB luciferase-reporter (Figure 2B). These data suggested that p50 has higher transactivation potential of VEGFR-3 promoter than p65 protein.

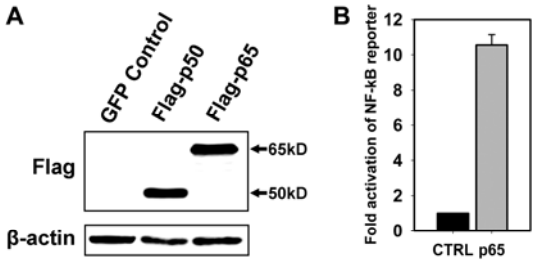

Figure 2. Equal expression of Flag-tagged NF-κB proteins and activation of the NF-κB-luciferase reporter by over-expression of Flag-p65. (A) HEK293 cells were seeded in 10cm^2 dishes and transfected with pCMV-Flag-p50 (0.5μg), pCMV-Flag-p65 (0.5μg), or control GFP expression vector (0.5μg). Following 48h incubation, cells were lysed and analyzed for Flag-protein expression by Western blot using anti-Flag antibodies. Note equal expression levels of both Flag-p50 and Flag-p65. (B) RLEC were seeded in a 24-well dish were co-transfected with a NF-κB-luciferase reporter plasmid and pCMV-Flag-p65 or empty vector control (0.5μg each plasmid). The next day, cells were lysed and reporter activity was measured by luciferase assay and normalized to total mg protein.

We used ChIP assay to determine whether NF-κB subunits bind putative targets identified on VEGFR-3 promoter. Primers were designed to encompass the region that includes (-238bp to -403bp) or lacks the potential sites. The -238/-403bp promoter segment containing the NF-κB sites was detected by anti-p50, anti-p65, and anti-acetylated-H3 antibodies, indicating binding and active transcription by NF-κB. ChIP analysis showed preferential binding by the p50 subunit (Figure 3B). Non-

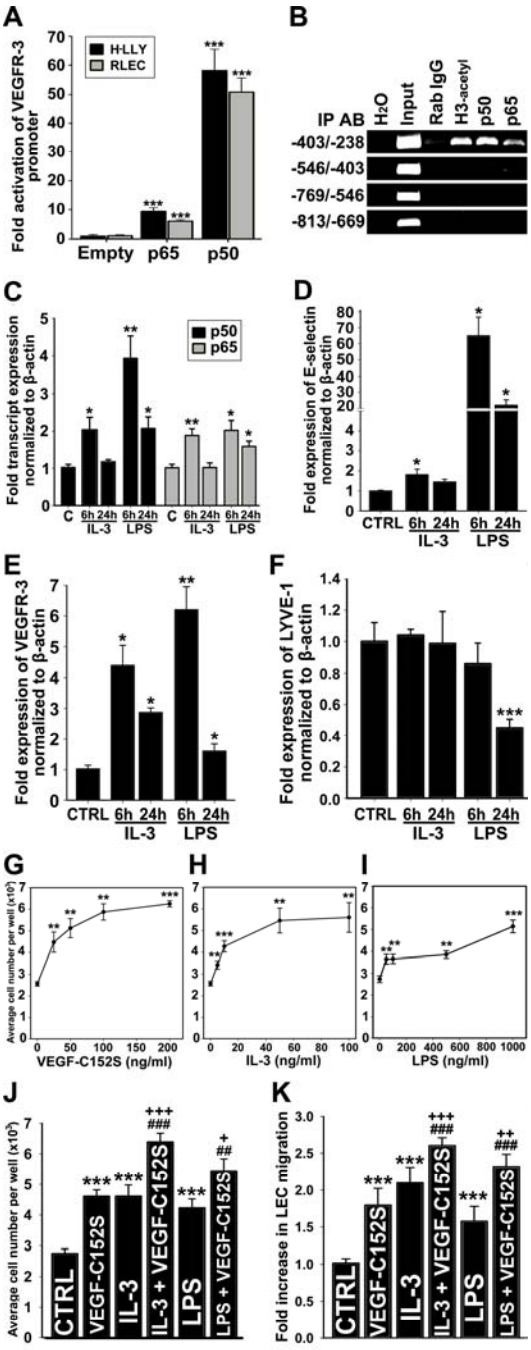

specific rabbit IgG and primers flanking the region devoid of NF-κB binding sites did not amplify PCR products, demonstrating specificity of the ChIP assay.

Inflammatory stimuli upregulate endogenous VEGFR-3 gene expression in LECs

Since the VEGFR-3 promoter was activated by NF-κB transcription factors, we reasoned that treatment of LECs with NF-κB dependent inflammatory mediators should increase the level of VEGFR-3 transcripts. To test this hypothesis, HDLEC$_{htert}$ were stimulated with known NF-κB activators, IL-3 (10ng/ml) or LPS (100ng/ml), for 6h and 24h, followed by qRT-PCR analysis of NF-κB p50 and p65, E-selectin, LYVE-1, and VEGFR-3 (Figures 3C-F). IL-3 and LPS were selected for initial studies because of the recently reported ability of IL-3 to induce expression of lymphatic-specific genes in cultured blood endothelial cells (BECs)[23] and the strong induction of lymphangiogenesis *in vivo* by LPS treatment[29]. In cultured LECs, IL-3 and LPS treatment for 6h or 24h activated NF-κB signaling as demonstrated by significant increase in p50, p65, and E-selectin, a known NF-κB-regulated gene (Figures 3C-D). A 6h exposure to LPS and IL-3 upregulated VEGFR-3 by

Figure 3. NF-κB pathway upregulates VEGFR-3 expression and activates lymphatic endothelial cells. (A) VEGFR-3 promoter activity in RLEC and H-LLY cells co-transfected with VEGFR-3$^{-849/+55}$ and pCMV-Flag-p50, pCMV-Flag-p65 or empty control plasmids. Promoter activity is normalized per mg of protein. Data presented for each cell line as the mean promoter activity ± SEM of three independent experiments performed in duplicate ± SEM (total n = 6 per experimental condition). *** denote *P*<.001 vs. control as determined by Student's unpaired t-test. (B) ChIP was performed using RLEC and anti-p65, -p50, -acetylated histone H3 antibodies (positive control), or non-specific rabbit IgG (negative control). Immunoprecipitated chromatin was visualized by PCR using primers either flanking (-403/-238bp) or upstrem of putative NF-κB binding sites (-813/-403bp). Data are representative of four independent ChIP experiments with similar results. (C, D, E, F) qRT-PCR analysis of NF-κB p50 and p65 (C), E-selectin (D), VEGFR-3 (E), and LYVE-1 (F) mRNA expression in HDLEC$_{htert}$ treated with IL-3 (10ng/ml) or LPS (100ng/ml) for 6h or 24h. The relative expression of each target was normalized to β-actin. Data are presented as the mean values of three independent experiments ± SEM. *P* values are indicated by **P*<.05, ***P*<.01, and ****P*<.001 vs. control as determined by Student's unpaired t-test. (G, H, I) RLEC proliferation induced by 72 hours exposure to VEGF-C152S (25-200 ng/ml) (G), IL-3 (5-100 ng/ml) (H) and LPS (50-1000 ng/ml) (I). (J) Additive proliferative effects of RLEC treated with VEGF-C152S (100 ng/ml), IL-3 (10 ng/ml), or LPS (500 ng/ml) alone as compared to pretreatment with IL-3 (10 ng/ml) or LPS (500 ng/ml) followed by stimulation with VEGF-C152S (100 ng/ml). (G, H, I, J) Data are presented as the average cell number of three independent experiments ± SEM (total n=6 per condition). (K) Migration of RLEC induced by treatment with VEGF-C152S (200 ng/ml), IL-3 (10 ng/ml), or LPS (500 ng/ml) and combined treatment with IL-3 (10 ng/ml) and VEGF-C152S (200 ng/ml) or LPS (500 ng/ml) and VEGF-C152S (200 ng/ml). RLEC migration towards 0.25% FBS was used as a negative control. Data presented as average fold increase in RLEC migration ± SEM of three independent experiments. *P* values for (J and K*)* are indicated as *<.05, **<.01, and ***<.001 vs. control. *P* values vs. cytokine treatment alone are indicated as $^{\#\#}$<.01 and $^{\#\#\#}$<.001. *P* values vs. VEGF-C152S treatment alone are indicated as $^{+}$<.05, $^{++}$<.01, and $^{+++}$<.001. All statistical tests were done by Student's unpaired t-test.

6.2±0.8- and 4.4±0.7-fold, respectively, whereas after 24h of treatment with these stimulators VEGFR-3 was upregulated by 1.6±2.4 and 2.9±0.2-fold (Figure 3E). In comparison, LYVE-1 was unchanged by IL-3 or downregulated after 24h of LPS treatment (Figure 3F) attesting to target specificity of NF-κB stimulation.

Inflammatory stimuli induce LEC proliferation and migration via VEGFR-3 signaling

The main goal of Task 1 was to determine the synergistic effects of inflammatory mediators on proliferation, migration and survival of LECs induced by VEGFR-3 ligands in vitro. Since both IL-3 and LPS upregulated VEGFR-3 gene expression in LECs, we hypothesized that IL-3 and LPS would enhance LEC proliferation and migration to VEGFR-3 specific ligands, such as, VEGF-C152S[30]. To test this hypothesis, we measured proliferation and migration of RLEC stimulated by IL-3 or LPS alone or in combination with VEGF-C152S. VEGF-C152S, IL-3, or LPS significantly increased RLEC proliferation in a dose-dependent manner, with maximum increase of 2.2-, 1.8-, and 2.4-fold compared with control, respectively (Figures 3G-I). Pre-activation with IL-3 or LPS followed 6h later by VEGF-C152S treatment significantly increased proliferation by 18-39% compared with individual

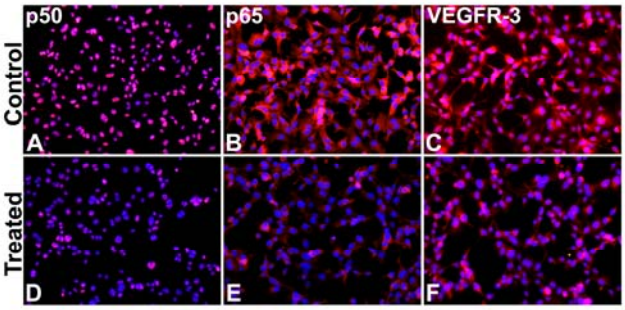

Figure 4. NF-κB inhibitor, PDTC, suppresses both constitutive NF-κB signaling and VEGFR-3 expression in LEC. RLEC cultured on slides were treated for 18h with either 1μM of the NF-κB inhibitor, PDTC, or vehicle. Cells were stained with antibodies against p50 (A, D), p65 (B, C), or VEGFR-3 (D, E). Note that inhibition of constitutive nuclear localization of NF-κB proteins coincided with decreased VEGFR-3 expression. Representative images from two independent experiments are shown.

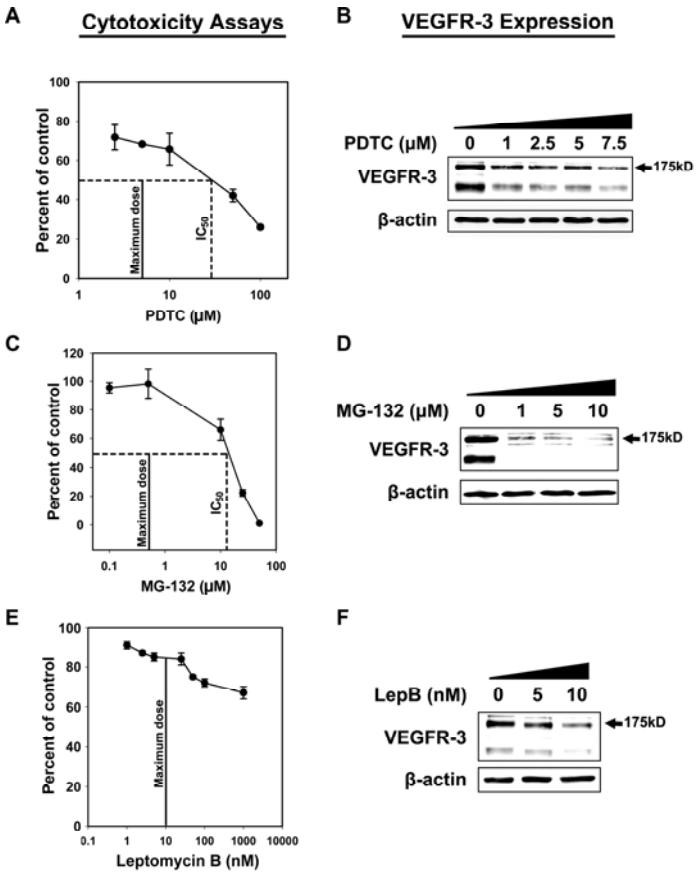

Figure 5. Dose-dependent suppression of VEGFR-3 protein expression by NF-κB inhibitors at doses below their IC_{50}. (A, C, E) RLEC were seeded at the density of 100,000 cells per well and treated with the indicated doses of PDTC, MG-132 and leptomycin B. The next day, cells were washed twice with PBS and trypsinized. Viable cells were identified by trypan blue exclusion method and enumerated. Maximal experimental doses (solid black lines) and IC_{50} concentrations (dashed lines) are shown on graphs for each inhibitor. Data presented as the mean percent of control ± SEM derived from triplicate wells. (B, D, F) RLEC were treated for 18-24 hours with the indicated doses of NF-κB inhibitors followed by assessment of VEGFR-3 expression by Western blot. All experiments were reproduced twice with similar results.

cytokines (Figure 3J). IL-3, LPS, or VEGF-C152S also induced RLEC migration by 2.1-, 1.6-, and 1.8-fold (Figure 3K). LEC migratory response to VEGF-C152S increased up to 44% after pre-treatment with IL-3 or LPS (Figure 3K). These results suggest that VEGFR-3 upregulation by inflammatory stimuli mediating NF-κB activation enhances LEC responsiveness to VEGFR-3 specific ligands.

Inhibition of NF-κB signaling represses VEGFR-3 expression in LECs

As outlined in Task 1, sub-aim A, we asked whether endogenous VEGFR-3 expression in LECs is maintained by constitutive NF-κB signaling. To answer this question, we determined the effects of an NF-κB inhibitor PDTC[31] on VEGFR-3 expression at the promoter, mRNA, and protein levels. PDTC treated LECs demonstrated a dose-dependent reduction (up to 60%) of VEGFR-3 promoter activity and mRNA (Figures 6A-B). Constitutive expression and nuclear localization of p50 and p65 were also inhibited by PDTC, which coincided with decreased VEGFR-3 expression (Figure 4). Neither cell viability (Figure 5) nor expression of NF-κB-independent targets (e.g., β-actin) was affected by PDTC at the tested concentrations (Figure 5B, insert). This effect was reproduced by two other inhibitors: MG-132, a blocker of IκB-α degradation[31], and leptomycin, an inhibitor of NF-κB nuclear transport[32]. Western blot showed up to 70%

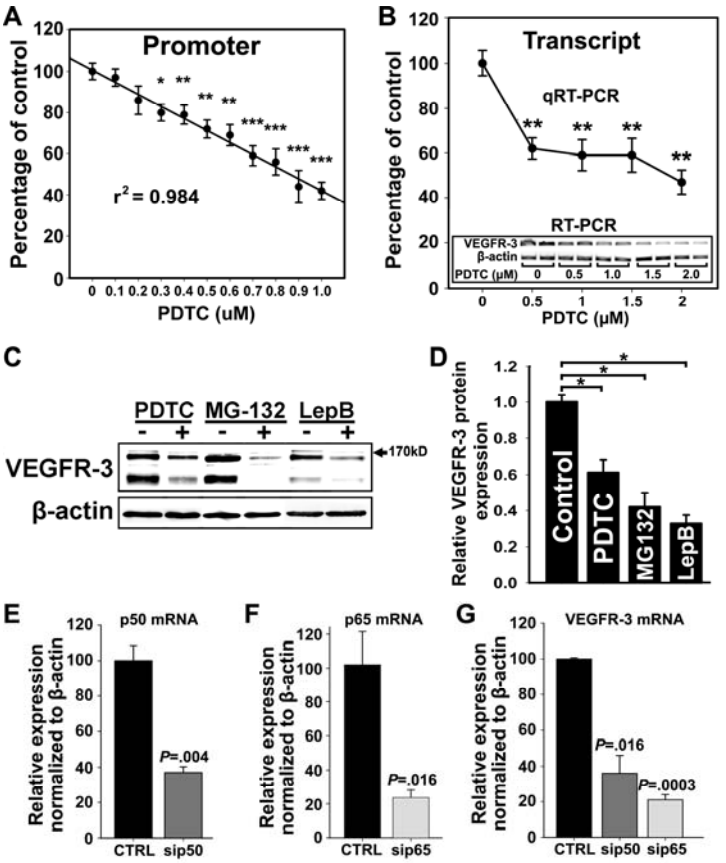

Figure 6. NF-κB signaling is required for VEGFR-3 expression in lymphatic endothelial cells (LECs). (A) RLEC were transfected with the full-length VEGFR-3$^{-849/+55}$ promoter and treated with PDTC (0-1μM) or vehicle for 18 hours. Promoter activity was measured by luciferase assay and normalized to total protein per well. Note linear inhibition of VEGFR-3 promoter activity by PDTC determined by linear regression (r^2 shown on graph) of the mean promoter activity ± SEM of three independent experiments performed in duplicate (total n = 6 per condition). (B) VEGFR-3 transcript expression assayed by qRT-PCR in RLEC treated with PDTC (0-2μM) or vehicle. Data are presented as mean transcript expression normalized to β-actin of three independent experiments ± SEM (total n = 3 per condition). Insert shows a dose-dependent decrease of VEGFR-3 transcript detected by RT-PCR. For B and C panels, *P* values are indicated by *<.05 vs. control, **<.01 vs. control, ***<.001 vs. control, by Student's unpaired t-test. (C) Western blot analysis of RLEC treated with PDTC (7.5μM), MG-132 (0.25μM), leptomycin B (10nM), or vehicle for 24 hours. β-actin was used as a loading control. (D) Densitometric values demonstrate a statistically significant decrease in VEGFR-3 protein normalized to β-actin from RLEC treated with NF-κB inhibitors or vehicle for 24 hours. Experiments were performed in duplicate and data are presented as mean β-actin normalized VEGFR-3 expression ± SEM. * indicates *P*<.05 vs. control, by Student's unpaired t-test. (E, F, G) H-LLY were transfected with p50 or p65 specific siRNA or scramble control siRNA for 48 hours and transcript expression for p50 (E), p65 (F), and VEGFR-3 (G) was determined by qRT-PCR. Data are presented as the mean transcript expression normalized to β-actin of three independent samples ± SEM (n = 3 per condition). Statistically significant differences were determined vs. control, by Student's unpaired t-test. *P*-values are displayed on the graphs.

reduction of VEGFR-3 expression by all inhibitors in a dose-dependent manner (Figures 5C-D). Drug concentrations that repressed VEGFR-3 protein expression were at least 10-fold below the IC_{50} values for LECs (Figure 5).

NF-κB regulation of VEGFR-3 expression was also confirmed by target-specific knockdown of NF-κB subunits. H-LLY were transfected with siRNA targeting p50 or p65 or scrambled control siRNA. qRT-PCR performed 48h after transfection showed 50-70% knockdown of p50 and p65 (Figures 6E-F) and a corresponding 50-80% reduction in VEGFR-3 transcripts (Figure 6G). Collectively, these data suggest that NF-κB is involved in regulation of endogenous VEGFR-3 expression.

Task 2. To determine the effect of deficient NF-κB signaling on VEGFR-3 expression, lymphangiogenesis and tumor metastasis in an orthotopic breast cancer model in female p50 knockout mice. To accomplish this task, we will:

A. Implant syngeneic breast carcinoma cell lines (one non-metastatic and one highly metastatic derivative sub-line) in the MFP of wild-type and NF-κB p50 knockout mice.
B. Assess the rate of tumor growth of both lines, tumor lymphangiogenesis, and lymphatic and distant metastasis.

Data toward accomplishment of Task 2

In this report we have accomplished the following preliminary studies necessary for completion of the goals outlined in Task 2:

- demonstrated that primary mediators of lymphangiogenesis, Prox1 and VEGFR-3, are elevated during inflammatory lymphangiogenesis *in vivo*
- characterized the expression of inflammatory and lymphangiogenic mediators using a time-course mouse model of inflammation

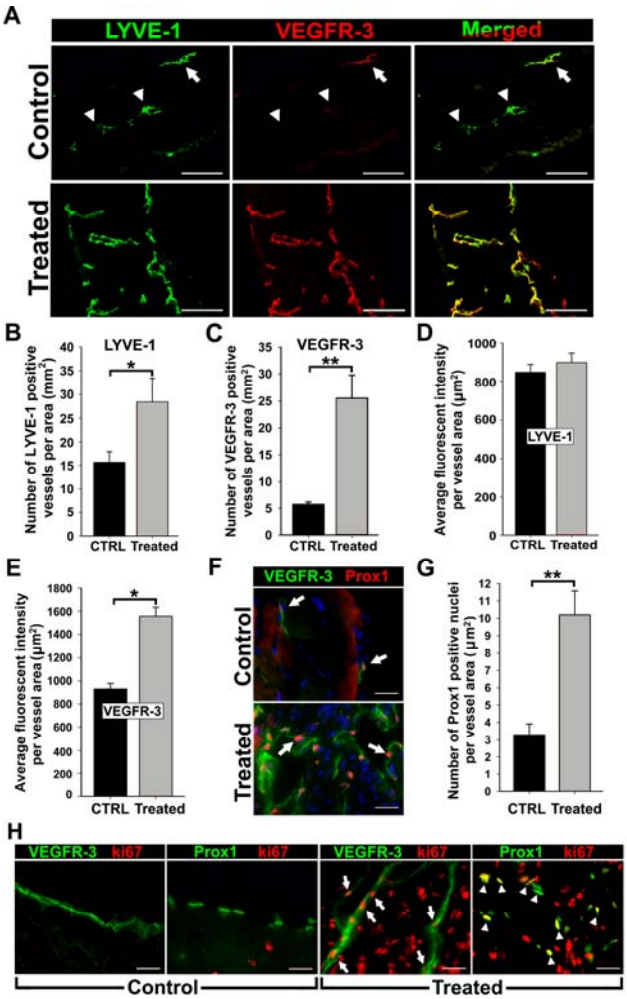

Figure 7. Inflammation induces VEGFR-3 and Prox1 expression in activated lymphatic vessels. Peritonitis was induced by repetitive i.p. injections of thioglycollate (TG) every 48h for two weeks. (A) Diaphragms from mice treated for 2 weeks with TG to induce peritonitis or saline as a control (n = 3 mice per group) were double stained with anti-LYVE-1 and anti-VEGFR-3 antibodies. Note strong expression and complete overlap of VEGFR-3 with LYVE-1 in inflamed tissues compared with quiescent lymphatic vessels in control sections with weakly detected (arrow) or absent (arrowheads) VEGFR-3. LYVE-1$^+$ (B) and VEGFR-3$^+$ (C) lymphatic vessels were counted on the entire diaphragm sections and the numbers were normalized per total section area expressed in mm^2. The results are presented as the mean vessel density per group ± SEM. For (B) * denotes *P*<.05 vs. control as determined by Wilcoxon rank sum test. For (C) ** indicate *P*<.01 vs. control as determined by Student's unpaired t-test. The mean fluorescent intensity (MFI) per vessel was analyzed on LYVE-1$^+$ (D) and VEGFR-3$^+$ (E) lymphatic vessels (5-10 vessels per diaphragm). MFI is expressed as relative units normalized per vascular area expressed in µm^2. The mean MFI values ± SEM derived from 3 mice per group are shown. For (E) * indicates *P*<.05 vs. control, as determined by nested ANOVA described in Methods. (F) Diaphragms from TG-treated and control mice were double-stained with anti-Prox1 and anti-VEGFR-3 antibodies. Arrows point to Prox1$^+$ nuclei. (G) Prox1$^+$ nuclei were enumerated and normalized per LYVE-1$^+$ lymphatic area (µm^2) in diaphragms of TG- and saline-treated control mice. ** indicates *P*<.01 vs. control as determined by Student's unpaired t-test. (H) Diaphragm sections were co-stained with antibodies against VEGFR-3 or Prox1 and a proliferative marker, Ki-67, to assess proliferative status of lymphatic vessels in the diaphragms of TG-treated or control mice. Note overlapping expression of Ki-67/VEGFR-3 (arrow) and Ki67/Prox1 (arrowhead) detected in inflamed lymphatic vessels but absent from quiescent lymphatic vessels in control tissues. Scale bars represent 100µm in panel A and 20µm in panels F, H.

- investigated whether VEGFR-3 upregulation is necessary for inflammation-induced angiogenesis.

The following data demonstrate that VEGFR-3 and Prox1 are key lymphangiogenic players that are upregulated by inflammation-induced NF-κB signaling *in vivo*. To study inflammatory lymphangiogenesis, we first performed preliminary studies in a non-tumorigenic model. This was applicable to Task 2 and necessary in order to first identify the functional role of specific inflammatory mediators in the absence of the complex tumor microenvironment. At the same time breast tumors are highly inflammatory in nature[1;2], suggesting that molecular mechanisms discovered in the non-tumorigenic thioglycollate model will likely be conserved in the tumor microenvironment. Execution of these studies has been planned for next year and will be greatly aided by the preliminary findings reported in the following section. Detailed methods for the following section of this report are found in Appendix 1.

Inflammation induces lymphatic expression of VEGFR-3 and Prox1 during lymphangiogenesis *in vivo*.

Regulation of VEGFR-3 by inflammation is suggested by reports demonstrating inhibition of lymphangiogenesis by blockade of VEGFR-3 signaling[10]. The lymphatic-specific transcription factor, Prox1, may also contribute to this process because it is induced by inflammatory mediators[23], which coincides with elevated VEGFR-3[33]. However, the roles of

VEGFR-3 and Prox1 in inflammatory lymphangiogenesis have not been demonstrated.

To analyze VEGFR-3 and Prox1 expression during inflammation, we induced peritonitis in Balb/c mice by TG injections, a reported method to induce lymphangiogenesis in the diaphragm[15]. Diaphragms from saline (control) and TG-treated mice were removed after a two-week treatment and stained for the lymphatic marker, LYVE-1, and VEGFR-3 (Figure 7). Consistent with previous studies[15;34], the number of LYVE-1$^+$ lymphatic vessels increased by 1.9±0.3-fold in TG-treated mice compared with controls (Figures 7A,B). These tissues also showed a 4.5±0.3-fold increase in VEGFR-3$^+$ vessel density (Figure 7C). Co-expression of VEGFR-3 and LYVE-1 was quantified using the method described by Tammela et al[35] that measures the fluorescent intensity of target expression normalized per vascular area. This revealed a lymphatic-specific increase of VEGFR-3 (~67%) but not LYVE-1 expression (Figures 7D-E), suggesting that inflammation increases both lymphatic vessel density and VEGFR-3 expression per individual vessel.

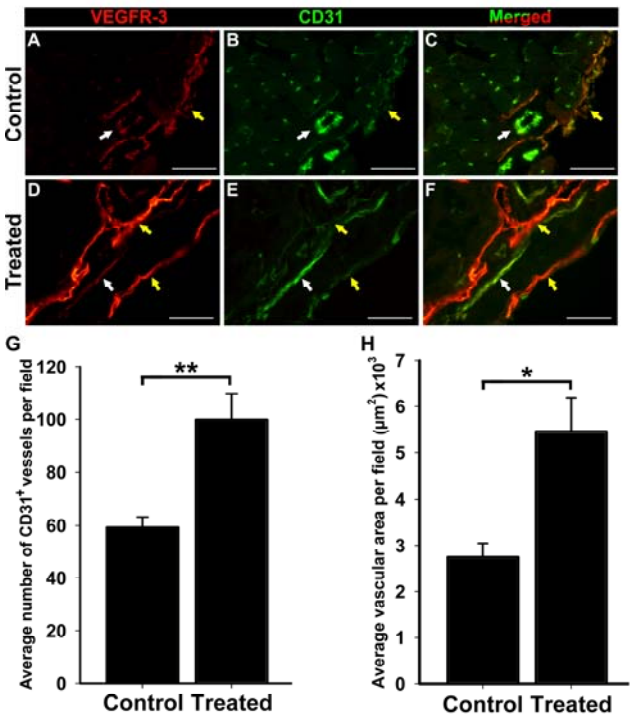

Figure 8. Angiogenesis is induced by inflammation but VEGFR-3 is not upregulated on CD31$^+$ blood vessels. Diaphragms from controls and mice treated with TG for 2 weeks (n=3 mice per group) were double-immunostained for VEGFR-3 (A, D) and the blood vessel marker CD31 (B, E). (C, F) VEGFR-3 was weakly expressed on a few CD31$^+$ blood vessels in both TG-treated and control diaphragms. Following TG-induced inflammation, VEGFR-3 was strongly upregulated on weakly stained CD31$^+$ lymphatic vessels (yellow arrows). In comparison, VEGFR-3 expression was not upregulated on strongly stained CD31$^+$ blood vessels in TG-inflamed tissues compared with control sections (white arrows). Scale bars = 100μm. (G) Blood vessel density and (H) total vascular area of CD31 stained diaphragm sections from controls and mice treated with TG for 2 weeks. (G) CD31$^+$ blood vessels were enumerated from 6 fields acquired at 40X magnification from 3 control and 3 treated mice. Data are presented as mean number of CD31$^+$ vessels per 40X field ± SEM. (H) CD31$^+$ vascular area was measured from 5 fields acquired at 40X magnification. To calculate vascular area per field, images were converted to binary images and blood vessels were outlined in black using ImageJ software. Data are presented as mean CD31$^+$ vascular density ± SEM. For (G, H) *p<0.05 and **p<0.01 vs. control, by Student's unpaired t-test.

Prox1 reportedly regulates VEGFR-3 expression in cultured LECs[19;21]; however, a similar function *in vivo* has not been reported. We sought to determine the status of Prox1 expression in VEGFR-3$^+$ lymphatic vessels during inflammation. Double-staining showed coincident upregulation of VEGFR-3 and Prox1 in lymphatic vessels of inflamed diaphragms as compared with control tissues (Figure 7F). Moreover, the frequency of Prox1$^+$ nuclei per lymphatic vessel area was increased by 3.3±0.5-fold (Figure 7G).

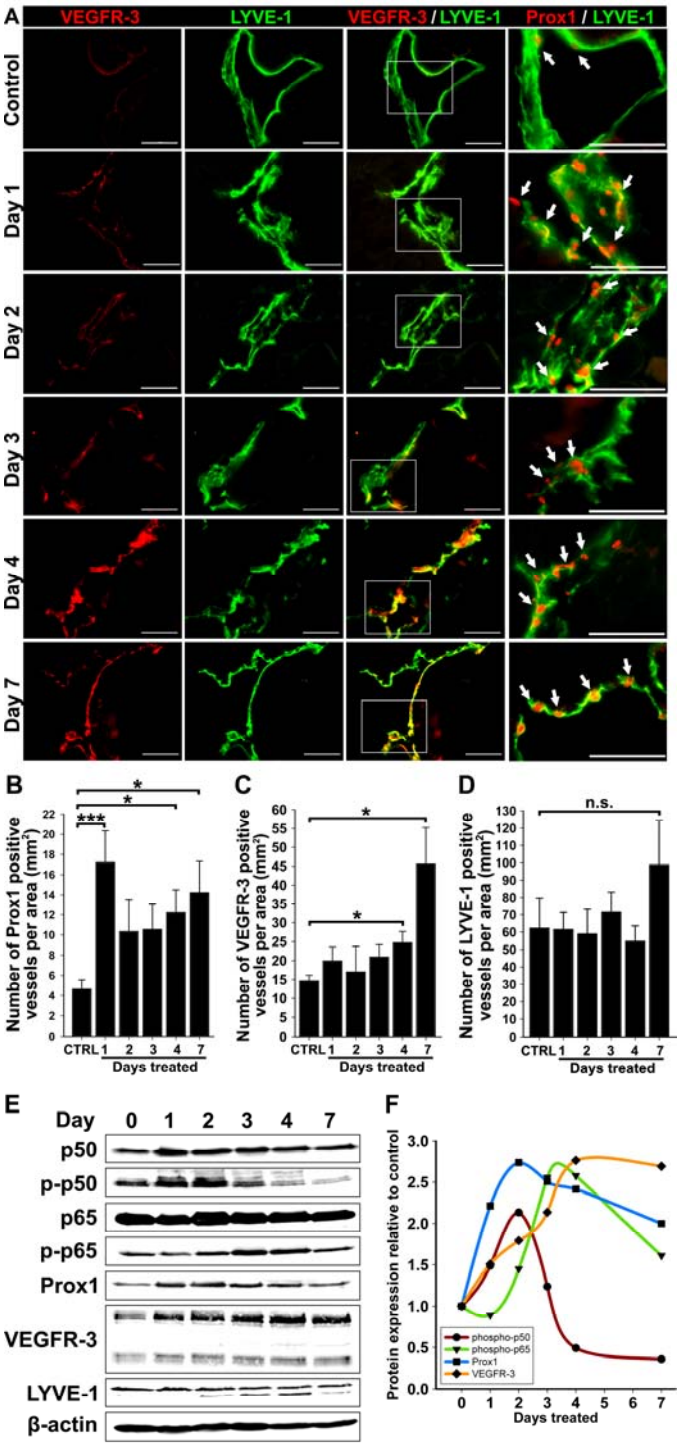

To determine the proliferative status of VEGFR-3$^+$/Prox1$^+$ vessels, control and inflamed sections were co-stained for Ki-67 in combination with anti-VEGFR-3 or anti-Prox1 antibodies. Quiescent lymphatic vessels of control mice lacked Ki-67. In contrast, diaphragm vessels in TG-treated mice displayed widespread Ki-67 colocalized with both Prox1 and VEGFR-3 (Figure 7H). Collectively, these data demonstrate that inflammation induces VEGFR-3 and Prox1 expression on pre-existing and sprouting lymphatic vessels.

Inflammation induces angiogenesis but does not upregulate VEGFR-3 on blood vasculature

VEGFR-3 expression and signaling are crucial for angiogenesis in some physiological settings, such as cancer[36] and corneal neovascularization[36]. Because angiogenesis is frequently induced by inflammation[37], we investigated whether VEGFR-3 upregulation was found on blood vessels as well as lymphatic vasculature. To assess the effect of inflammation on angiogenesis and on VEGFR-3 expression in blood vascular endothelial cells, we double-stained control and inflamed tissues (n = 5 per group) with anti-VEGFR-3 antibody and an antibody

Figure 9. Upregulation of VEGFR-3 and Prox1 precedes new lymphatic vessel formation during inflammation. (A) Double immunostaining of VEGFR-3/LYVE-1 and Prox1/LYVE-1 in serial diaphragm sections derived from mice treated with saline or TG (n = 3-4 mice per group) and harvested 1, 2, 3, 4 and 7 days after onset of treatment. Lymphatic vessels shown are representative of whole diaphragm sections. Scale bars represent 50 µm. Lymphatic vessels shown are representative of whole diaphragm sections from 3-4 mice per group. Panels B, C, and D show quantification of Prox1 (B), VEGFR-3 (C), and LYVE-1 (D) positive vessels normalized per area of the entire diaphragm section measured in mm^2. Quantitative analysis was performed on diaphragms harvested from 3-4 mice per group at indicated days after the first TG or saline injection. Data are presented as the mean number of vessels per diaphragm section ± SEM; n.s. denotes non-significant changes; * and ** indicate *P*<.05 and *P*<.01 vs. control, respectively, as determined by Student's unpaired t-test. (E) Protein expression of Prox1, VEGFR-3, LYVE-1, NF-κB p50 phosphorylated on Ser-337, non-phosphorylated NF-κB p50, NF-κB p65 phosphorylated on Ser-276, non-phosphorylated NF-κB p65, and β-actin was determined by Western blot of combined lysates (100µg of total protein per lane) derived from 3-4 mice per group. (F) Protein expression in Western blots was determined by band densitometry. Values were normalized to β-actin and are shown as fold increase relative to expression of corresponding proteins in untreated control mice at day 0.

specific for the blood vascular endothelial marker CD31. The results showed that VEGFR-3 is weakly expressed on some CD31 vessels on both control and inflamed tissues following 2 weeks of TG-treatment. However, the level of VEGFR-3 expression was unchanged on CD31-positive vessels (Figure 8B,E) while it was clearly increased on LYVE-1 positive vessels (Figure 8A,C). This discrepancy is particularly noticeable on merged Figure 9F that shows side-by-side high VEGFR-3 expression on a lymphatic vessel lacking CD31 marker and barely detectable VEGFR-3 on a parallel $CD31^+$-vessel. Despite the fact that VEGFR-3 expression did not significantly change on $CD31^+$ vessels between control and treated tissues, both density and blood vascular area identified by $CD31^+$ marker increased during inflammation by 68% and 98%, respectively (Figure 8G,H). We, therefore, concluded that although inflammation promotes formation of both blood and lymphatic vessels, up-regulation of VEGFR-3 was primarily associated with lymphangiogenesis because it occurred specifically in the lymphatic endothelial cells.

Increased Prox1 and VEGFR-3 expression precedes lymphangiogenesis

LEC activation is associated with increased Prox1[38] and VEGFR-3[6], yet their lymphatic-specific expression kinetics at early stages of lymphangiogenesis has not been examined. To determine the timeline of events leading to lymphangiogenesis, diaphragms from control and TG-treated mice (3-4 per group) harvested at days 1-4 and 7 post-treatment were analyzed for expression of Prox1, VEGFR-3, and LYVE-1 by immunofluorescence and Western blot. Figures 9A-B show that compared with control tissues, the density of $Prox1^+$ lymphatic vessels increased (3.8-fold, $P<.001$) on the first day and remained significantly elevated (2.2- to 3.1-fold) on days 2-7. In contrast, the increase in $VEGFR\text{-}3^+$ vessel density became statistically significant only on day 4 (1.7-fold, $P<.05$) and day 7 (3.1-fold, $P<.01$, Figure 2C). During this period, $LYVE\text{-}1^+$ vessel density was unchanged except an insignificant 1.6-fold increase on day 7 (Figure 9D). This immunofluorescent analysis showed that increased Prox1 expression precedes VEGFR-3 up-regulation by 2-3 days and elevation of both proteins precedes lymphangiogenesis.

Table 1. Fold increase of β-actin normalized protein expression relative to day 0 control

Target Protein \ Day	0	1	2	3	4	7
p50	1.00	**1.93**	1.81	1.77	1.75	1.62
p-p50	1.00	1.49	**2.13**	1.24	0.49	0.36
p65	1.00	0.95	1.24	1.28	**1.39**	1.33
p-p65	1.00	0.89	1.45	2.55	**2.58**	1.61
Prox1	1.00	2.21	**2.73**	2.51	2.42	2.00
VEGFR-3	1.00	1.51	1.79	2.14	**2.76**	2.69
LYVE-1	1.00	0.96	1.15	1.11	**1.42**	0.90

Densitometric values for diaphragm lysates from mice treated with TG for 0-7 days, corresponding to the western blots shown in Figure 9E. Peak values for each target protein are boxed.

Western blot analysis of actin-normalized protein expression of lymphatic markers as well as total and phosphorylated NF-κB p50 and p65 at different days post-treatment confirmed this conclusion (Figure 9E). As expected, p50, p65, p-p50 and p-p65 were induced by inflammation with the most pronounced changes detected in p-p50 on the first day of treatment. Increase in NF-κB was mirrored by Prox1 expression kinetics that doubled on day 1 of inflammation and nearly tripled on day two (Figure 9F). In contrast, the peak of VEGFR-3 expression was delayed to day 4 on which its level in inflamed tissues was 2.8-fold higher compared with controls (Table 2). Consistent with immunostaining, no changes in LYVE-1 protein were detected over 7 days of treatment. These data suggest that activation of NF-κB, possibly in conjunction with Prox1, might be responsible for LEC activation, leading to VEGFR-3 elevation and lymphangiogenesis. Because no significant changes in LYVE-1$^+$ vessel density were detected in the first week of inflammation, these findings imply that NF-κB, Prox1 and VEGFR-3 are all required for lymphangiogenesis that is preceded by upregulation of these proteins by 3-5 days.

The VEGFR-3 promoter is activated by Prox1

The role of Prox1 in postnatal lymphangiogenesis associated with breast cancer or inflammation has not been well defined. However, Prox1 has been reported to induce VEGFR-3 expression in cultured endothelial cells[19;21] and elevated VEGFR-3 expression and signaling correlates strongly to increased tumor lymphangiogenesis and lymphatic metastasis[18]. This evidence and our data demonstrating that Prox1 is elevated by inflammation (Figures 8,9), which preceded induction of both VEGFR-3 elevation and lymphangiogenesis suggests that Prox1 may specifically and directly regulate lymphangiogenesis through VEGFR-3 promoter activation. However, Prox1 regulates more than 90 genes[21] and transactivation of the VEGFR-3

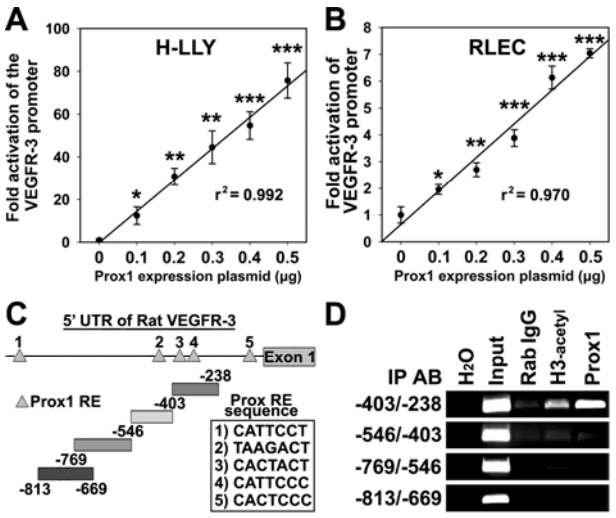

Figure 10. Prox1 directly activates the VEGFR-3 promoter. VEGFR-3$^{-849/+55}$ promoter plasmid was co-transfected with pCMV-Prox1 plasmid (0-0.5μg) in H-LLY (A) and RLEC (B). Promoter activity was measured by luciferase assay and normalized per mg protein. Note linear response to Prox1 transactivation in both cell lines as determined by linear regression (r^2 shown on graph) of mean promoter activity ± SEM of three independent experiments performed in duplicate (n = 6 per condition) (A, B). For panels A and B, *P* values are indicated as * <.05 vs. control, **<.01 vs. control, ***<.001 vs. control, by Student's unpaired t-test. (C) Schematic presentation of putative Prox1 response elements in rat promoter of VEGFR-3. Also shown are sequences and locations of Prox1 response elements in relation to the rat VEGFR-3 transcriptional start site. (D) ChIP analysis of the VEGFR-3 promoter was performed on RLEC as described in legend for Figure 4. Immunoprecipitated chromatin was visualized by PCR with primers flanking transcription factor binding sites (-403/-238bp) or upstream of binding sites (-813/-403bp). Data are representative of three independent ChIP experiments with similar results.

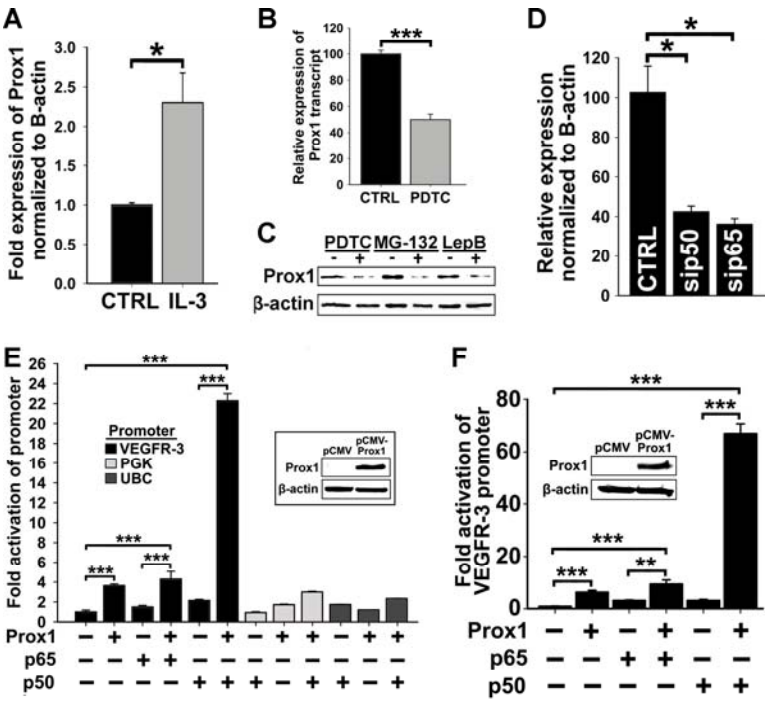

Figure 11. The p50 subunit of NF-κB upregulates Prox1, and both p50 and Prox1 synergistically regulate VEGFR-3 expression. (A) qRT-PCR analysis of Prox1 transcripts in $HDLEC_{htert}$ treated with IL-3 (10ng/ml) for 6h. (B) qRT-PCR analysis of Prox1 transcripts in RLEC treated with PDTC (2.5μM) for 24h. In both (A, B) data are presented as β-actin normalized mean transcript expression of three independent experiments performed in duplicate ± SEM (total n = 6 per condition). (C) Prox1 detected by Western blot of nuclear extracts from RLEC treated with PDTC (5μM), MG-132 (250nM), leptomycin B (10nM), or vehicle alone. β-actin was used as a loading control. Representative data are shown from one of three experiments. (D) qRT-PCR analysis of Prox1 transcript in H-LLY transfected with p50 and p65 siRNA. Data are presented as the mean transcript expression normalized to β-actin ± SEM derived from three independent samples. (E) Prox1-negative non-endothelial line HEK293 was transfected with VEGFR-$3^{-849/+55}$ promoter expression and pCMV-Flag-p50 or pCMV-Flag-p65 plasmids and co-transfected with pCMV-Prox1 or empty vector (0.25μg of each plasmid). VEGFR-3 promoter activity was normalized to total mg of protein. Insert confirms lack of Prox1 in control HEK293 and forced-expression in transfected cells. Activation of VEGFR-3 promoter by co-expression of p50 and Prox1 was compared with the effect on NF-κB-independent promoters for phosphoglycerate kinase (PGK) and Ubiquitin C (UBC) examined under the same conditions. Data presented as the mean promoter activity ± SEM of three independent experiments performed in triplicate (total n = 9 per condition). (F) Prox1-negative blood vascular endothelial line, HULEC, was transfected with VEGFR-$3^{-849/+55}$ promoter expression and pCMV-Flag-p50 or pCMV-Flag-p65 plasmids and co-transfected with pCMV-Prox1 or empty vector, as described under 7E. The analysis of the VEGFR-3 promoter activity was performed as under 7E. Data are presented as the mean VEGFR-3 promoter activity ± SEM derived from three independent experiments performed in quadruplicate (total n = 12 per condition). The *P* values for all experiments are indicated as *<.05, **<.01, and ***<.001 vs. control, as determined by Student's unpaired t-test.

promoter by Prox1 has not been previously shown. To determine whether Prox1 transcriptionally regulates VEGFR-3, LECs were co-transfected with VEGFR-$3^{-849/+55}$ promoter and escalating concentrations (0-0.5μg) of a Prox1-encoding or empty vector followed by measurement of luciferase activity. Relative to empty-vector control, overexpression of Prox1 increased VEGFR-$3^{-849/+55}$ activity in a linear dose-dependent manner by 7-fold and 76-fold in RLEC and H-LLY, respectively (Figures 10A-B).

Several putative Prox1 binding sites, analogous to published consensus sequences (CA/tc/tNNCT/c and TA/tAGNC/tN[39]), are present in the either human or rat VEGFR-3 promoter (rat sequences shown in Figure 10C). ChIP assay in RLEC showed that the region containing consensus Prox1 binding sites (-403/-238bp) was immunoprecipitated by anti-Prox1 antibody (Figure 10D). Prox1 antibodies did not pulled-down other flanking promoter DNA, indicating specific interaction between Prox1 and the VEGFR-3 promoter under steady state conditions. Collectively, these data suggest that both NF-κB and Prox1 bind VEGFR-3 promoter and activate its transcription.

NF-κB regulates Prox1 expression in LECs

We found that forced expression of Prox1 activated VEGFR-3 promoter *in vitro* and both Prox1 and VEGFR-3 are induced by inflammation *in vivo* with Prox1 upregulation preceding that of VEGFR-3 (Figure 9). This suggested that NF-κB might first upregulate Prox1 followed by cooperative regulation of VEGFR-3. To test this hypothesis, the level of Prox1 expression was quantified by qRT-PCR following 6h stimulation by IL-3 (10ng/ml), conditions which increased VEGFR-3 expression (Figure 3E). IL-3 treatment significantly increased Prox1 by 2-fold (P<.01, Figure 11A), implicating Prox1 as a downstream target of NF-κB.

We next investigated the effects of NF-κB inhibitors on Prox1 expression. PDTC suppressed Prox1 mRNA by ~60% (Figure 11B), suggesting that Prox1 transcription requires NF-κB. Western blot showed that PDTC, MG-132 and leptomycin all significantly repressed Prox1 expression (Figure 11C). Moreover, p50 and p65 targeting but not scrambled siRNA also decreased Prox1 expression by 60% (Figure 11D), corroborating the hypothesis that NF-κB regulates Prox1 in LECs.

Prox1 and NF-κB synergistically activate the VEGFR-3 promoter

Cultured LECs express high levels of Prox1 and p50 making it difficult to evaluate the contributions of either factor to VEGFR-3 transcription. To test whether Prox1 and NF-κB cooperate in activation of the VEGFR-3 promoter, we used non-endothelial and endothelial Prox1-negative lines (HEK293 and HULEC). Similar results were obtained in both lines co-transfected with Prox1 (Figures 11E-F, inserts), the full-length VEGFR-3$^{-849/+55}$ promoter and Flag-p50, Flag-p65 or empty vector. In the absence of Prox1, p50 weakly activated the VEGFR-3 promoter while p65 had no effect. Combination of Prox1 and p65 did not increase promoter activity compared with Prox1 alone. In contrast, combination of Prox1 and p50 activated the VEGFR-3 promoter 22.3±0.7-fold and 66.9±3.8 over the vector control in HEK293 and HULEC, respectively (Figures 11E-F). Combination of Prox1 and p50 had no effect on the activity of NF-κB-independent ubiquitin C (UBC) or phosphoglycerate kinase (PGK) promoters. These results suggest that Prox1 and NF-κB p50 specifically cooperate to activate the VEGFR-3 promoter in a synergistic manner during inflammation.

Task 3. To determine the effect of anti-inflammatory treatment on VEGFR-3 expression, tumor lymphangiogenesis, lymphatic metastasis, and spread to distant organs in an orthotopic model of human breast carcinoma, MDA-MB-231. To accomplish this task, we will:

A. Implant luciferase tagged human breast carcinoma line MDA-MB-231 into the MFP of CB-17 SCID mice and treat them with NF-κB targeting anti-inflammatory drugs, PDTC and dexamethasone.
B. Assess tumor growth, tumor lymphangiogenesis, and lymphatic metastasis to distant organs.

Execution of this aim is scheduled for the next year. The analysis of this aim is likely to be completed in the third year of the proposal.

Key research accomplishments

Year 1 Annual Report

- Cloned and characterized nine human VEGFR-3 promoter-reporter constructs ranging from -849bp to -46bp relative to the transcription start site
- Identified NF-κB subunits p50 and p65 as key regulators of the VEGFR-3 promoter *in vitro* by using ChIP and promoter-reporter analyses
- Identified the lymphatic-specific transcription factor, Prox1, as a direct activator of the VEGFR-3 promoter *in vitro* by using ChIP and promoter-reporter analyses
- Discovered using a time-course model of inflammatory lymphangiogenesis that expression of Prox1 is rapidly increased by 1-2 days after the onset of inflammation and this is followed a 3-fold in VEGFR-3 protein expression 2-3 days later
- Found that upregulation of both Prox1 and VEGFR-3 precedes inflammation-induced formation of new lymphatic vessels
- Determined that the NF-κB dependent inflammatory stimuli, IL-3 and LPS, increase VEGFR-3 transcript expression by 4- to 6-fold
- Showed that increased VEGFR-3 expression in response to inflammatory mediators increases LEC responsiveness of to VEGFR-3 specific ligands.

Reportable outcomes

Year 1 Annual Report

Manuscripts in review:

1. **Michael J. Flister**, Andrew Wilber, Kelly L. Hall, Caname Iwata, Kohei Miyazono, Riccardo E. Nisato, Michael S. Pepper, David C. Zawieja and Sophia Ran. Inflammation induces lymphangiogenesis through upregulation of VEGFR-3 mediated by NF-κB and Prox1. Under revision with *Blood*.

2. Sophia Ran, Lisa Volk, Kelly Hall, and **Michael J. Flister** (January 2009). Lymphangiogenesis and Lymphatic Metastasis in Breast Cancer. Under revision with *Pathophysiology*.

Presentations:

1. 2nd Place Presentation in 19th Annual Trainee Symposium, SIU School of Medicine, May 2009.

2. Selection for oral presentation, "VEGFR-3 and Prox1 are elevated by NF-κB during inflammatory lymphangiogenesis" Tumor biology: Mechanistic Approaches to Targeting Angiogenesis Minisymposium, American Association for Cancer Research Annual Meeting, Denver, CO, April 2009.

Abstracts:

1. **Flister M.J.** and Ran S. VEGFR-3 and Prox1 are elevated by NF-κB during inflammatory lymphangiogenesis. 2nd Place Presentation in 19th Annual Trainee Symposium, SIU School of Medicine, May 2009.

2. **Michael J. Flister**, Andrew Wilber, Kelly L. Hall, Caname Iwata, Kohei Miyazono, Riccardo E. Nisato, Michael S. Pepper, David C. Zawieja, and Sophia Ran. VEGFR-3 and Prox1 are elevated by NF-κB during inflammatory lymphangiogenesis. American Association for Cancer Research Annual Meeting, Denver, CO, April 2009

Conclusion

Here we have presented the first molecular evidence that VEGFR-3, the central mediator of lymphangiogenesis, is directly regulated by NF-κB transcription factors, p50 and p65, in response to extracellular inflammatory stimuli. We also present novel evidence that the lymphatic-specific transcription factor Prox1 is induced by NF-κB-dependent inflammation and elevation of both NF-κB and Prox1 preceded upregulation of VEGFR-3 by 2-3 days *in vivo* (**Figures 7,9**). *In vitro* we demonstrated that NF-κB and Prox1 transcription factors directly transactivate the VEGFR-3 promoter (**Figure 3,10**). Moreover, our data show that NF-κB dependent mediators, IL-3 and LPS, increased Prox1 and VEGFR-3 expression and responsiveness of LECs to the VEGFR-3 specific ligand, VEGF-C152S (**Figure 3**). Collectively, these results suggest that LEC stimulation by NF-κB-dependent cytokines amplifies the lymphangiogenic signals by increasing VEGFR-3 expression. Listed below are the key findings of this report:

(1) NF-κB dependent inflammation significantly increased VEGFR-3 protein expression (2.8-fold) VEGFR-3^{+} vessel density by 2.8- and 3.1-fold, respectively (**Figure 9**)

(2) Inflammation rapidly increased phosphorylated NF-κB p50 by 2.1-fold, which coincided with a 2.2 to 2.7-fold increase Prox1 expression by days 1-2. Importantly, upregulation both transcription factors preceded increases in VEGFR-3 expression by 2-3 days (**Figure 9 and Table 1**).

(3) The VEGFR-3 promoter was directly transactivated in human LECs by co-transfection with Prox1 (76±8-fold), p50 (58±7-fold), or p65 (9±1.0-fold), while siRNA and pharmacalogical inhibitors targeting NF-κB significantly repressed VEGFR-3 transcipts by 60-70% (**Figures 3,6,10**).

(4) Significant 4- to 6-fold elevation of VEGFR-3 transcripts in LECs treated with known NF-κB activating inflammatory stimuli, IL-3 and LPS either for 6h or 24 h (**Figure 6**).

(5) Inflammatory stimuli also increased LEC proliferation and migration by 1.8- to 2.4-fold and 1.6- to 2.1-fold, correspondingly, and enhanced LEC activation by the VEGFR-3-specific ligand, VEGF-C152S by 20-40% (**Figure 6**).

The key findings of this study suggest a central mechanism underlying tumor-induced inflammation, lymphangiogenesis and metastasis, and present Prox1 and VEGFR-3 as potential new targets for anti-metastatic therapy in the treatment of breast cancer patients.

Reference List

1. Ben Baruch A. Host microenvironment in breast cancer development: inflammatory cells, cytokines and chemokines in breast cancer progression: reciprocal tumor-microenvironment interactions. Breast Cancer Res. 2003;5:31-36.

2. Yu JL, Rak JW. Host microenvironment in breast cancer development: inflammatory and immune cells in tumour angiogenesis and arteriogenesis. Breast Cancer Res. 2003;5:83-88.

3. Schoppmann SF, Horvat R, Birner P. Lymphatic vessels and lymphangiogenesis in female cancer: mechanisms, clinical impact and possible implications for anti-lymphangiogenic therapies (Review). Oncol.Rep. 2002;9:455-460.

4. Mouta C, Heroult M. Inflammatory triggers of lymphangiogenesis. Lymphat.Res.Biol. 2003;1:201-218.

5. Chakrabarti R, Subramaniam V, Abdalla S, Jothy S, Prud'homme GJ. Tranilast inhibits the growth and metastasis of mammary carcinoma. Anticancer Drugs 2009;20:334-345.

6. Veikkola T, Jussila L, Makinen T et al. Signalling via vascular endothelial growth factor receptor-3 is sufficient for lymphangiogenesis in transgenic mice. EMBO J. 2001;20:1223-1231.

7. Kaipainen A, Korhonen J, Mustonen T et al. Expression of the fms-like tyrosine kinase 4 gene becomes restricted to lymphatic endothelium during development. Proc.Natl.Acad.Sci.U.S.A 1995;92:3566-3570.

8. Whitehurst B, Flister MJ, Bagaitkar J et al. Anti-VEGF-A therapy reduces lymphatic vessel density and expression of VEGFR-3 in an orthotopic breast tumor model. Int.J.Cancer 2007;121:2181-2191.

9. Paavonen K, Puolakkainen P, Jussila L, Jahkola T, Alitalo K. Vascular endothelial growth factor receptor-3 in lymphangiogenesis in wound healing. Am.J.Pathol. 2000;156:1499-1504.

10. Baluk P, Tammela T, Ator E et al. Pathogenesis of persistent lymphatic vessel hyperplasia in chronic airway inflammation. J.Clin.Invest 2005;115:247-257.

11. Kunstfeld R, Hirakawa S, Hong YK et al. Induction of cutaneous delayed-type hypersensitivity reactions in VEGF-A transgenic mice results in chronic skin inflammation associated with persistent lymphatic hyperplasia. Blood 2004;104:1048-1057.

12. Zhang Q, Lu Y, Proulx ST et al. Increased lymphangiogenesis in joints of mice with inflammatory arthritis. Arthritis Res.Ther. 2007;9:R118.

13. Maruyama K, Ii M, Cursiefen C et al. Inflammation-induced lymphangiogenesis in the cornea arises from CD11b-positive macrophages. J.Clin.Invest 2005;115:2363-2372.

14. Cursiefen C, Chen L, Borges LP et al. VEGF-A stimulates lymphangiogenesis and hemangiogenesis in inflammatory neovascularization via macrophage recruitment. J.Clin.Invest 2004;113:1040-1050.

15. Iwata C, Kano MR, Komuro A et al. Inhibition of cyclooxygenase-2 suppresses lymph node metastasis via reduction of lymphangiogenesis. Cancer Res. 2007;67:10181-10189.

16. Ristimaki A, Narko K, Enholm B, Joukov V, Alitalo K. Proinflammatory cytokines regulate expression of the lymphatic endothelial mitogen vascular endothelial growth factor-C. J.Biol.Chem. 1998;273:8413-8418.

17. Goldman J, Rutkowski JM, Shields JD et al. Cooperative and redundant roles of VEGFR-2 and VEGFR-3 signaling in adult lymphangiogenesis. FASEB J. 2007;21:1003-1012.

18. Roberts N, Kloos B, Cassella M et al. Inhibition of VEGFR-3 activation with the antagonistic antibody more potently suppresses lymph node and distant metastases than inactivation of VEGFR-2. Cancer Res. 2006;66:2650-2657.

19. Hong YK, Harvey N, Noh YH et al. Prox1 is a master control gene in the program specifying lymphatic endothelial cell fate. Dev.Dyn. 2002;225:351-357.

20. Wigle JT, Harvey N, Detmar M et al. An essential role for Prox1 in the induction of the lymphatic endothelial cell phenotype. EMBO J. 2002;21:1505-1513.

21. Petrova TV, Makinen T, Makela TP et al. Lymphatic endothelial reprogramming of vascular endothelial cells by the Prox-1 homeobox transcription factor. EMBO J. 2002;21:4593-4599.

22. Mishima K, Watabe T, Saito A et al. Prox1 induces lymphatic endothelial differentiation via integrin alpha9 and other signaling cascades. Mol.Biol.Cell 2007;18:1421-1429.

23. Groger M, Loewe R, Holnthoner W et al. IL-3 induces expression of lymphatic markers Prox-1 and podoplanin in human endothelial cells. J.Immunol. 2004;173:7161-7169.

24. Karin M. Nuclear factor-kappaB in cancer development and progression. Nature 2006;441:431-436.

25. Beinke S, Ley SC. Functions of NF-kappaB1 and NF-kappaB2 in immune cell biology. Biochem.J. 2004;382:393-409.

26. Kiriakidis S, Andreakos E, Monaco C et al. VEGF expression in human macrophages is NF-kappaB-dependent: studies using adenoviruses expressing the endogenous NF-kappaB inhibitor IkappaBalpha and a kinase-defective form of the IkappaB kinase 2. J.Cell Sci. 2003;116:665-674.

27. Tsai PW, Shiah SG, Lin MT, Wu CW, Kuo ML. Up-regulation of vascular endothelial growth factor C in breast cancer cells by heregulin-beta 1. A critical role of p38/nuclear factor-kappa B signaling pathway. J.Biol.Chem. 2003;278:5750-5759.

28. Iljin K, Karkkainen MJ, Lawrence EC et al. VEGFR3 gene structure, regulatory region, and sequence polymorphisms. FASEB J. 2001;15:1028-1036.

29. Kang S, Lee SP, Kim KE et al. Toll-like receptor 4 in lymphatic endothelial cells contributes to LPS-induced lymphangiogenesis by chemotactic recruitment of macrophages. Blood 2009;113:2605-2613.

30. Kirkin V, Mazitschek R, Krishnan J et al. Characterization of indolinones which preferentially inhibit VEGF-C- and VEGF-D-induced activation of VEGFR-3 rather than VEGFR-2. Eur.J.Biochem. 2001;268:5530-5540.

31. Dai Y, Rahmani M, Grant S. Proteasome inhibitors potentiate leukemic cell apoptosis induced by the cyclin-dependent kinase inhibitor flavopiridol through a SAPK/JNK- and NF-kappaB-dependent process. Oncogene 2003;22:7108-7122.

32. Walsh MD, Jr., Hamiel CR, Banerjee A et al. Exportin 1 inhibition attenuates nuclear factor-kappaB-dependent gene expression. Shock 2008;29:160-166.

33. Kilic N, Oliveira-Ferrer L, Neshat-Vahid S et al. Lymphatic reprogramming of microvascular endothelial cells by CEA-related cell adhesion molecule-1 via interaction with VEGFR-3 and Prox1. Blood 2007;110:4223-4233.

34. Oka M, Iwata C, Suzuki HI et al. Inhibition of endogenous TGF-{beta} signaling enhances lymphangiogenesis. Blood 2008;111:4571-4579.

35. Tammela T, Saaristo A, Lohela M et al. Angiopoietin-1 promotes lymphatic sprouting and hyperplasia. Blood 2005;105:4642-4648.

36. Tammela T, Zarkada G, Wallgard E et al. Blocking VEGFR-3 suppresses angiogenic sprouting and vascular network formation. Nature 2008;454:656-660.

37. Li X, Massa PE, Hanidu A et al. IKKalpha, IKKbeta, and NEMO/IKKgamma are each required for the NF-kappa B-mediated inflammatory response program. J.Biol.Chem. 2002;277:45129-45140.

38. Srinivasan RS, Dillard ME, Lagutin OV et al. Lineage tracing demonstrates the venous origin of the mammalian lymphatic vasculature. Genes Dev. 2007;21:2422-2432.

39. Chen X, Taube JR, Simirskii VI, Patel TP, Duncan MK. Dual roles for Prox1 in the regulation of the chicken betaB1-crystallin promoter. Invest Ophthalmol.Vis.Sci. 2008;49:1542-1552.

40. Wilber A, Frandsen JL, Wangensteen KJ et al. Dynamic gene expression after systemic delivery of plasmid DNA as determined by in vivo bioluminescence imaging. Hum.Gene Ther. 2005;16:1325-1332.

41. Whitehurst B, Eversgerd C, Flister M et al. Molecular profile and proliferative responses of rat lymphatic endothelial cells in culture. Lymphat.Res.Biol. 2006;4:119-142.

42. Nisato RE, Harrison JA, Buser R et al. Generation and characterization of telomerase-transfected human lymphatic endothelial cells with an extended life span. Am.J.Pathol. 2004;165:11-24.

43. Laderach D, Compagno D, Danos O, Vainchenker W, Galy A. RNA interference shows critical requirement for NF-kappa B p50 in the production of IL-12 by human dendritic cells. J.Immunol. 2003;171:1750-1757.

44. Surabhi RM, Gaynor RB. RNA interference directed against viral and cellular targets inhibits human immunodeficiency Virus Type 1 replication. J.Virol. 2002;76:12963-12973.

Appendix A

Materials and Methods

Materials – Human Prox1 CDS ligated into pCMV6-XL6 (pCMV-Prox1) plasmid was purchased from OriGene (Rockville, MD). NF-κB plasmids, pCMV-Flag-p50 and pCMV-Flag-p65, were kindly provided by Dr. Baldwin (University of North Carolina, Chapel Hill, NC). Promoter-luciferase reporter plasmids for ubiquitin C and phosphoglycerate kinase were described previously[40]. Lipopolysaccharide (LPS) was purchased from Sigma-Aldrich (St. Louis, MO). Rat VEGFR-3 specific ligand, VEGF-C152S, and human interleukin-3 (IL-3) were purchased from Peprotech (Rocky Hill, NJ). Pyrrolidine dithiocarbamate (PDTC) and MG-132 were purchased from Calbiochem (San Diego, CA). Leptomycin B was from LC Laboratories (Woburn, MA).

Antibodies – Primary antibodies used in this study were: goat anti-mVEGFR-3 and anti-Prox1 (R&D Systems, Minneapolis, MN); rabbit anti-p65, anti-pp65, anti-p50, and anti-pp50 (Santa Cruz, Santa Cruz, CA); rabbit anti-mLYVE-1 and anti-Prox1 (AngioBio, Del Mar, CA); rabbit anti-Ki-67 (Biomeda, Foster City, PA); goat anti-acetylated-histone-H3 (Upstate Temecula, CA); mouse anti-Flag (ABM, Richmond, BC, Canada); mouse anti-β-actin (JLA20) (Developmental Studies Hybridoma Bank, Iowa City, IA); and rabbit anti-VEGF-C (Invitrogen, Carlsbad, CA). Secondary HRP-, FITC- and Cy3-conjugated donkey anti-rabbit and anti-goat antibodies and non-specific rabbit IgG were from Jackson ImmunoResearch Laboratories, (West Grove, PA).

Cell lines – Rat lymphatic endothelial cells (RLEC) were isolated and cultured as previously described[41]. Human embryonic kidney cells (HEK293) were cultured in DMEM with 10% FBS. Human primary lymphatic endothelial cells (H-LLY) and immortalized human dermal lymphatic endothelial cells ($HDLEC_{htert}$)[42] were cultured in gelatin-coated flasks in EGM2 medium (Clonetics, San Diego, CA). Human lung microvascular endothelial cells (HULEC) were obtained from the Center for the Disease Control (Atlanta, GA).

Mouse peritonitis model - Female BALB/c mice (3 to 6 months) were obtained from Jackson Laboratory (Bar Harbor, ME) and treated in accordance with institutional guidelines. Peritonitis was induced by 0.5ml intraperitoneal (i.p.) injections of 1.5% BBL sodium thioglycollate (v/v in saline) (BD Biosciences, Franklin Lakes, NJ) for 2 weeks, as previously described[15]. For time-course analysis of inflammatory lymphangiogenesis, mice (3-4 per group) received thioglycollate (TG) every 48h for the indicated periods. Control mice were injected i.p. with 0.5ml saline. Diaphragms were removed after a 2-week treatment, fixed with 10N Mildform for 1h at room temperature, bathed in 30% sucrose overnight and snap-frozen.

Immunohistochemistry – Frozen 8-µm sections were fixed with acetone for 10min, washed in PBST (pH 7.4, 0.1% Tween-20) for 10min and incubated for 1h at 37^0C with primary antibodies (diluted 1:100) against anti-VEGFR-3, LYVE-1, Prox1, or Ki-67, followed by appropriate FITC or Cy3-conjugated secondary antibodies (diluted 1:100) for 1h at 37^0C. For double immunofluorescent staining, sections were incubated with each primary and secondary antibody for 1h at 37^0C and washed for 10min in PBST between steps. Slides were mounted in Vectashield medium containing 4,6'-diamidino-2-phenylindole (DAPI) nuclear stain (Vector Labs, Orton Southgate, U.K.). Images were acquired on an Olympus BX41 upright microscope equipped with a DP70 digital camera and DP Controller software (Olympus, Center Valley, PA).

Immunofluorescent intensity measurements – Analysis of VEGFR-3 and LYVE-1 double-staining was performed as described by Tammela *et al*[35], with slight modifications. In brief, diaphragm sections were double-stained with goat anti-mVEGFR-3 and rabbit anti-mLYVE-1 antibodies. Fluorescent images were acquired at a constant exposure time using a 400X objective on an Olympus IX71 inverted microscope (Olympus, Center Valley, PA) equipped with a Retiga Exi charge-coupled device camera (QImaging, Surrey, BC, Canada). Diaphragms stained with secondary antibodies alone were used to set the exposure time. Images acquired at a constant exposure time were converted to 12-bit gray scale followed by outlining vascular structures and analysis with Image-Pro Software (Media Cybernetics, Silver Springs, MD). Figure S1 shows an example of image acquisition and vessel outlining. All images were within a linear fluorescent intensity range between 0 and 4095. To exclude non-specific staining, structures less than 10µm (1µm = 6.4 pixels) in diameter were excluded. To calculate mean vessel intensity, the sums of pixel intensities per vessel were divided by total vessel area (μm^2). Mean vessel intensities from 5-10 images per diaphragm (n=3 per group) were averaged and compared between treated and control groups.

Western blot analysis – Cells were lysed in ice-cold buffer (50mM Tris-HCl, pH 7.5, 150mM NaCl, 1mM EDTA, 1% Triton-X100, 0.1% SDS, PMSF 1:100, and protease inhibitor cocktail 1:50). Proteins were separated in 12% SDS-polyacrylamide gel and transferred onto nitrocellulose membranes followed by overnight incubation with primary antibodies against p50, p65, Prox1, LYVE-1, VEGFR-3, Flag-tag, or β-actin; 1h incubation with HRP-conjugated secondary antibodies and development with ECL (Pierce, Rockford, IL). Protein bands were visualized using a Fujifilm LAS-3000 camera and analyzed with Image-Reader LAS-3000 software (Valhalla, NY).

VEGFR-3 promoter cloning – Segments of -849bp, -514bp, -341bp, -331bp, -118bp, and -46bp of the 5'UTR of VEGFR-3 and +55bp of exon1 were amplified by PCR from a human genomic BAC clone, CTD-2546M13 (Open Biosystems, Huntsville, AL). Additionally, Δ309 lacking the transcription start site (-849bp/-254bp) was created as a negative control. Products were cloned into the pGL4 Basic vector (Promega, Madison, WI) to produce VEGFR-3 promoter-luciferase constructs. All clones were sequenced and verified through comparison to published genomic sequence. Human VEGFR-3 promoter sequence (GenBank accession DQ911346) was analyzed using MatInspector (www.genomatix.de/products/MatInspector/index.html) and compared to published transcription factors binding sites.

Assay for VEGFR-3 promoter activity – Cells were transfected using 3μl of ExGen500 per well (Fermentas, Hanover, MD) with 1μg DNA comprised of 0.96μg promoter construct and 0.04μg of *Herpes simplex* thymidine-kinase promoter driven renilla luciferase (Promega, Madison, WI). After 24h, cells were lysed with 0.2% Triton-X100 in DPBS, and firefly and renilla luciferase activities were measured by a dual-luciferase assay performed according to manufacturer's protocol (Promega, Madison, WI). Promoter-firefly luciferase activity was normalized by renilla activity or mg of total protein.

Inflammatory stimulation of LECs – $HDLEC_{htert}$ were seeded in 6-well plates (200,000 cells/well) in 0.5% EGM2 media (Lonza, Basel, Switzerland). Medium was replaced daily during 72h prior to treatment with IL-3 (10ng/ml) or LPS (100ng/ml) for 6h or 24h. RNA extraction and analysis of transcript expression by qRT-PCR was performed as described below.

Cell proliferation and migration assays - RLEC were seeded in DMEM containing 1.5% of FBS in 24-well plates at the density of 50,000 cells/well. IL-3 (5-100ng/ml), LPS (50-1000ng/ml) and VEGF-C152S (25-200ng/ml) were added 2h after seeding. The effect of the combined cytokines was measured following stimulation with VEGF-C152S (100ng/ml) mixed with IL-3 (10ng/ml) or LPS (500ng/ml). Following 72h incubation, cells were washed, trypsinized, and enumerated. The results are presented as the averaged cell number per well derived from three experiments performed in triplicate ± SEM.

Cell migration was measured using 8μm-pore Transwells according to the manufacturer's protocol (Corning, Lowell, MA). In brief, 50,000 RLEC were seeded in 0.25% DMEM on pre-equilibrated inserts. IL-3 (10ng/ml), LPS (500ng/ml), VEGF-C152S (200ng/ml), or 0.25% FBS (negative control) were added to bottom

chambers. Following 24h incubation, inserts were washed, fixed in 2% paraformaldehyde for 10min and stained by crystal violet. Numbers of cells migrated-per-field were determined on 6 random images acquired at 200X and averaged.

Chromatin Immunoprecipitation (ChIP) – RLEC ($2x10^7$) were grown to 90% confluence and fixed with 1% formaldehyde. Cell lysis, shearing, and ChIP were performed using a ChIP-IT Express Kit according to manufacturer's protocol (Active Motif, Carlsbad, CA). Chromatin was precipitated with anti-p50, p65, Prox1, acetylated-histone-H3 antibodies, or non-specific rabbit IgG (negative control). Precipitated chromatin was amplified by PCR using primers for rat VEGFR-3 promoter listed in Table S1.

Suppression of p50/p65 expression by siRNA – Previously validated 21-nt-long siRNA duplexes against p50 (sense-strand 5'-GGGGCUAUAAUCCUGGACUdTdT-3')[43] and p65 (sense-strand 5'-GCCCUAUCCCUUUACGUCAdTdT-3')[44] (Dharmacon, Lafayette, CO) and pre-designed Silencer Negative Control #1 siRNA (cat. AM4611, Ambion) were used for suppression of p50 and p65 expression. H-LLY cells were transfected with siRNA for 16h using siPORT NeoFX (Ambion, Austin, TX) according to the manufacturer's protocol. Total RNA was isolated 48h post-transfection and transcript levels were determined by qRT-PCR.

RT-PCR and qRT-PCR – Total RNA extracted by Tri-reagent was reverse transcribed using RTG You-Prime Reaction beads (Amersham, Piscataway, NJ) and random hexamer primers (Invitrogen, Carlsbad, CA). All primers used in this study are listed in Table S1. Endpoint RT-PCR analysis was performed as previously described[8], then visualized and analyzed using a FluroChem5500 imaging system (AlphaInnotech, San Leandro, CA). QRT-PCR was performed using SYBR Master Mix and 7500 Real-Time PCR machine from Applied Biosystems (Foster City, CA). Data were normalized to β-actin and relative mRNA expression was determined using the ΔΔCt method.

Statistical analysis – Statistical analysis was performed using SAS software (SAS Institute, Inc., Cary, NC). All results are expressed as mean ± SEM. Differences in lymphatic vessel densities between groups were assessed by unpaired Student's *t*-test or Wilcoxon rank sum test. Intensity of VEGFR-3 and LYVE-1 staining per lymphatic vessels were assessed by ANOVA for a nested design. Statistical significance was defined as $P<.05$.